Novel Applications of Tetrazoles Derived from the TMSN3-Ugi Reaction

Zhao, Ting

Chapter 7

Bioisosteric replacement of carboxyl group with tetrazolyl moiety suggests a new avenue for designing human arginase inhibitors

Abstract

A nonclassical bioisosteric replacement of carboxyl group with tetrazolyl moiety at α position of 2-amino-6-boronohexanoic acid (ABH) results in novel human arginase inhibitors. Herein, tetrazolyl-containing human arginase inhibitors were successfully synthesized using multicomponent reaction. The relevant pharmacokinetic and X-ray crystallography results of the synthetic arginase inhibitors are presented. We found that the lead compound **1b-**2 possesses a moderate inhibitory potency for human arginase I and II, compared to that of ABH.

Ting Zhao, Sergey Lunev, Matthew Grove, Herman Meurs, Alexander Dömling,
In preparation.

7.1 Introduction

Arginase is a binuclear manganese metalloenzyme which catalyzes the hydrolysis of L-arginine, resulting in ornithine and urea.[1] Two isozymes are identified in mammals: arginase I (hArg I) and II (hArg II).[2] They are encoded by different genes and possess different tissue distributions, subcellular localizations, and metabolic functions.[3] Arginase I is a cytosolic isozyme, mainly found in liver where it catalyzes the final step of the urea cycle,[4] whereas arginase II is a mitochondrial isozyme, predominantly expressed in extrahepatic tissues such as kidney, brain, lactating mammary gland, gastrointestinal tract, and red blood cells.[4-7] Although the physiological function of arginase II is currently not fully understood, it is generally acknowledged that arginase II plays a key role in hemostasis of ornithine that is the precursor for the biosynthesis of polyamines and proline.[8, 9]

In NO producing cells, arginase competes for a common substrate, L-arginine, with nitric oxide synthase (NOS). The overexpression of arginase could reduce the level of L-arginine and, consequently, decrease the bioavailability of nitric oxide (NO). NO is widely recognized as an important intracellular signal transmissioner in many physiological functions including vasodilation, inhibiting platelet aggregation, preventing neutrophil/platelet adhesion to endothelial cells, inhibiting smooth muscle cell proliferation and migration, regulating programmed cell death (apoptosis), and maintaining endothelial cell barrier function.[10] In addition, in the respiratory tract, NO regulates the muscle relaxation of airway and vascular smooth muscle tone, and inflammatory processes involved in the host defense against invading microorganisms and malignant cells.[11-16] Furthermore, the upregulation of arginase is observed in the clitoral corpus cavernosum and vagina of patients suffering from sexual arousal disorders, as the NO deficiency affects the NO-dependent relaxation of smooth muscle which is required for erection.[7, 17]

On the other hand, the hydrolytic product ornithine could be converted to polyamines and proline by subsequent enzymatic reactions. Proline is relevant with collagen formation which for example induces the airway remodeling in asthma, while polyamines facilitate the repair of inflammatory lesions and cell proliferation.[18] It shall be noted that an abnormal exaggeration of polyamines in an aging cardiovascular system might induce endothelial dysfunction in both heart and vasculature.

At present, the effective upregulation of L-arginine is a prevalent strategy to treat NO-deficiency induced diseases. The simplest way might be the external administration of L-

arginine, which however did not induce a higher NOS activity. This is due to the fact that arginase shows a ~1000 times higher hydrolytic rate to L-arginine than NOS, although NOS possesses a higher affinity with L-arginine.[19] Meanwhile, the inhibition of arginase activity would be a better approach, by utilizing potent arginase inhibitors.

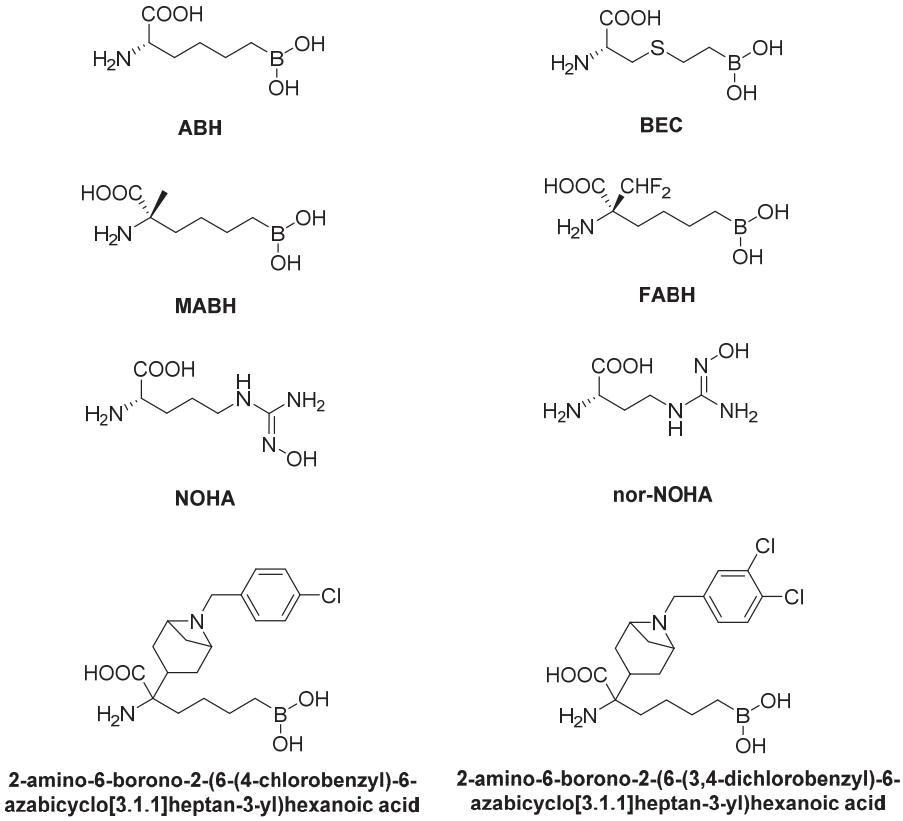

Figure 7.1 Structures of some reported Arginase I and II inhibitors.

Up until now, many potent human arginase inhibitors have been developed (Figure 7.1).[17, 20-28] The most distinguishing work has been pioneered by Christianson *et al*.[20] They firstly resolved the X-ray crystal structure of the ternary arginase-ornithine-borate complex, which provided a better understanding of the inhibition mode. Later they found that the tetrahedral borate anion of protease inhibitors can mimic binding interactions postulated for the tetrahedral transition states.[29] Based on these, they introduced a boronic acid moiety to replace the guanidino group of L-arginine, which afforded an L-arginine analogue 2(*S*)-amino-6-boronohexanoic acid (ABH), a potent, noncompetitive inhibitor for human arginase. Moreover, they revealed the crystal structure of human arginase I-ABH complex, which further proved that the high affinity of ABH for human arginase is derived from the aforementioned tetrahedral intermediate (and flanking transition states) for arginase-catalyzed hydrolysis of L-arginine.

Recently, Schroeter *et al.* identified the α position of ABH as an excellent site for introducing novel substituents that could provide additional bindings with enzymes.[30] Moreover, they synthesized a series of α,α-disubstituted ABH derivatives functioning as arginase inhibitors. Among these new inhibitors, 2-amino-6-borono-2-(6-(4-chlorobenzyl)-6-azabicyclo[3.1.1]heptan-3-yl)hexanoic acid and 2-amino-6-borono-2-(6-(3,4-dichlorobenzyl)-6-azabicyclo[3.1.1]heptan-3-yl)hexanoic acid possess the highest inhibitory potency for human arginase as reported in the literature up until now.

Currently, the bioisosteric replacement of carboxyl group with tetrazolyl moiety has been widely used in drug design. This replacement could be a new design route towards novel arginase inhibitors. Given the fact that tetrazolyl moiety possesses a higher hydrophobicity and metabolism stability, the introduction of tetrazole can possibly avoid some unfavorable absorption, distribution, metabolism, and excretion (ADME) properties. Furthermore, the nitrogen rich tetrazole can provide more potential binding sites for interacting with the amino acid residues of proteins.

In this work, we started with the synthesis of tetrazole-containing ABH analogues as novel and promising potent arginase inhibitors using Ugi reaction followed by deprotection. Ugi reaction is referred to one of multicomponent reactions in which more than two starting materials are converted to one product.[31-33] Multicomponent reactions are a powerful tool towards the one-pot synthesis of diverse and complex compounds in a short time, for example 'drug-like' heterocycles which are difficult to synthesize via classical methods. To the best of our knowledge, Ugi reaction is rarely employed to synthesize arginase inhibitors. Our study suggests a new avenue for the development of human arginase inhibitors.

Furthermore, we tested the inhibitory potency of the prepared compounds for human arginase by enzyme assay at physiological conditions. For the lead compound, the crystal structure with human arginase was investigated by X-ray Crystallography, to understand the affinity with amino acid residues of human arginase.

7.2 Inhibitor design and synthesis

We employed isocyanide based Ugi reaction to prepare a library of compounds in one-pot, by simply mixing the starting materials aldehyde, amine, azidotrimethylsilane ($TMSN_3$) and isocyanide in methanol with moderate to excellent yields (Scheme 7.1, the concentration of each was 1 M). After deprotection, three series of ABH analogues were produced: unsubstituted

tetrazole containing ABH analogues, tetrazole containing ABH analogues with substituted amino groups, and ABH analogues with 1-substituted tetrazole. The results are summarized in Tables 7.1 – 7.3.

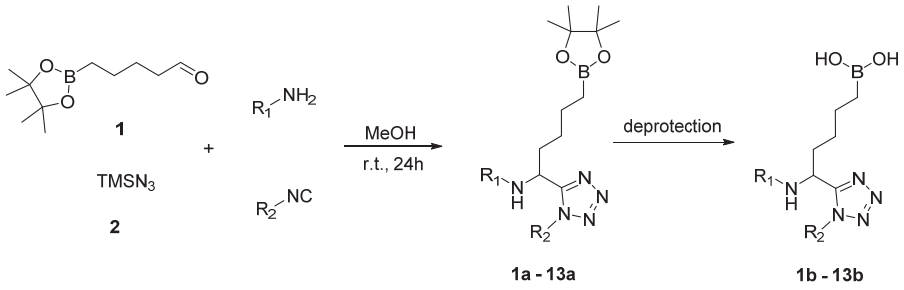

Scheme 7.1. Synthesis of tetrazole containing ABH analogues.

Table 7.1. Yields of Ugi products and unsubstituted tetrazole containing ABH analogues

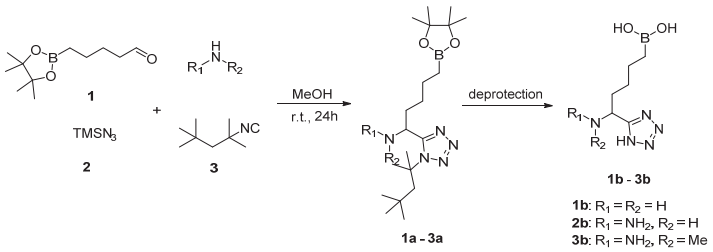

Entry	R_1	Ugi product a	Yield [%]	Unsubstituted tetrazole containing ABH analogues b	Yield [%]
1	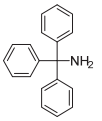	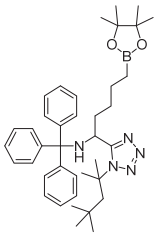	67	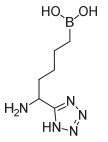	60
2	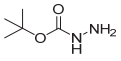	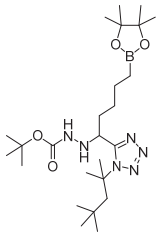	53	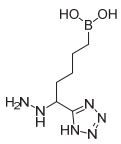	78
3	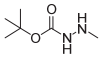	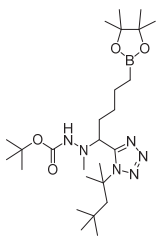	88	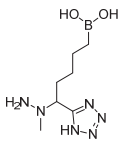	58

Table 7.2. Yields of Ugi products and tetrazole containing ABH analogues with substituted amino group

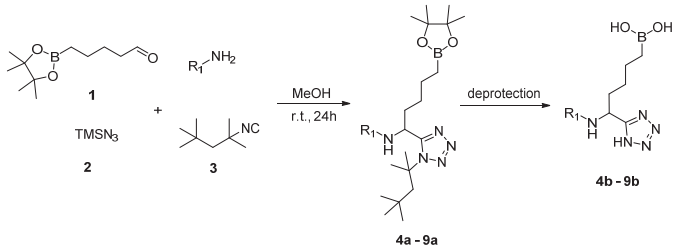

Entry	R_1	Ugi product a	Yield [%]	tetrazole containing ABH analogues with substituted amino group b	Yield [%]
4		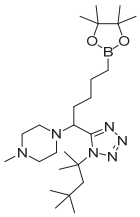	67	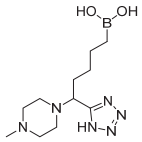	81
5		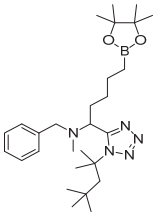	82	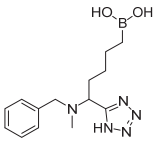	66
6		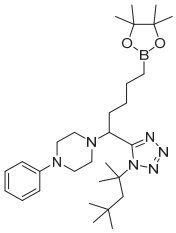	75	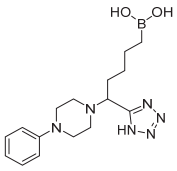	74
7		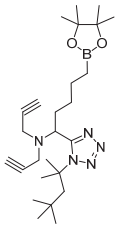	79	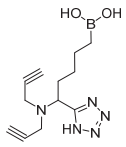	78
8	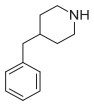	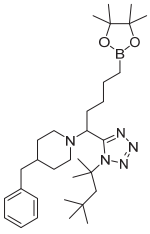	87	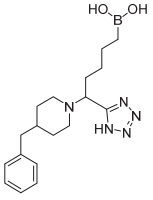	56

9		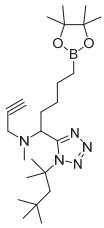	61	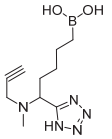	89

Table 7.3. Yields of Ugi products and ABH analogues with 1-substituted tetrazole

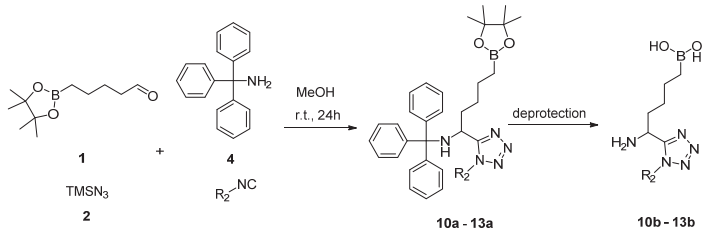

Entry	R_2	Ugi product a	Yield [%]	ABH analogues with 1-substituted tetrazole b	Yield [%]
10	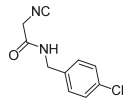	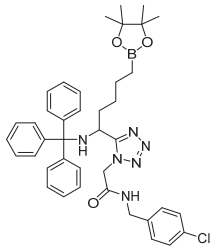	65	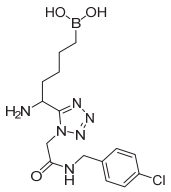	96
11		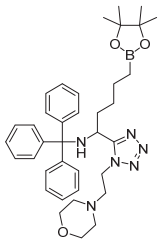	28	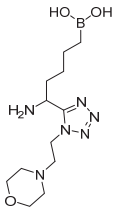	82
12	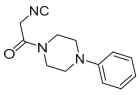	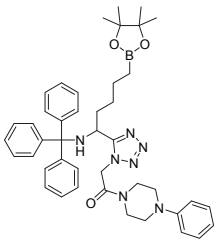	40	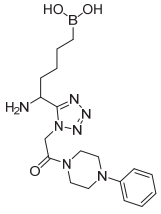	60
13		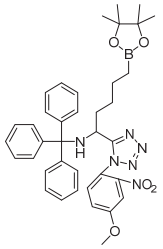	72	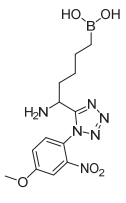	90

It should be pointed out that tritylamine was employed as an amino resource to prepare the Ugi products for unsubstituted tetrazole containing ABH analogue **1a** and all Ugi products for ABH analogues with 1-substituted tetrazole **10a** – **13a**, as it can be easily cleaved under acidic condition. These Ugi reactions proceeded smoothly at room temperature, which did not require high energy input by microwave irradiation. This is in contrast with our previous finding which showed the failure of Schiff base formation when tritylamine was used as the amine resource.[34] In this work, the possible explanation for the successful Schiff base formation at room temperature might be the higher reactivity of aldehyde **1** due to the presence of boronate.

7.3 Results and discussion

The lack of stereo-selectivity is a well-established feature of Ugi reaction. The inhibitory potency of compound **1b**, a racemic mixture, was tested for human arginase I and II using the reported method.[30, 35] Noteworthy, the activity of arginase is pH dependent, and the highest experimental activity was observed at a pH of 9.0 – 9.5. To better mimic the inhibiting behavior of the tested compound in vivo, we decided to perform our enzyme assay at pH of 7.4 which is more physiologically relevant. As shown in Table 7.4, the tetrazole bioisosteric analogue **1b** (racemic mixture) did not show any improvement in inhibitory potency compared with ABH. As reported in literature, the recognition of the amino acid residues of arginase requires strict stereochemical constraints for inhibitors, and only L-arginine can be the hydrolytic substrate of arginase instead of D-arginine.[36] Probably only one enantiomers of compound **1b** can interact with human arginase and inhibit human arginase activity. In order to investigate the true inhibitory potency of tetrazole containing inhibitor, the racemic mixture of compound **1b** needs to be separated into two enantiomers with the absolute conformation for each. Unfortunately, we failed to separate two enantiomers of compound **1b** by chiral chromatography. However, compound **1a**, a racemic mixture, is the precursor of compound **1b**, could be easily separated. Therefore, we prepared two enantiomers of **1a** followed by an acidic deprotection for each, which resulted in two enantiomers of compound **1b**: **1b**-1 and **1b**-2. Their inhibitory potency for human arginase I and II is summarized in Table 7.5. Clearly, compound **1b**-2 showed a great increase in inhibitory potency for human arginase I and II, compared with compound **1b** (racemic mixture), but no improvement compared with that of ABH.

Table 7.4. Inhibition of recombinant human arginase I and II by tetrazole containing ABH analogues

Tested compound	Inhibition (IC_{50})[a]	
	hArg I	**hArg II**
ABH	690 nM	460 nM
1b (racemic mixture)	150.83 μM	69.50 μM
2b	-[a]	-[a]
3b	-[a]	-[b]
4b	94826 μM[c]	-[b]
10b	-[a]	-[a]

[a] The IC_{50} cannot be determined using the tested maximum concentration of inhibitor; [b] The enzyme assay was not performed; [c] The enzyme assay was performed at pH = 10.5.

Table 7.5. Inhibition of recombinant human arginase I and II by **1b** (racemic mixture) and two enantiomers **1b-**1 and **1b-**2

Tested Compound	Inhibition (IC_{50})[a]	
	hARG I	**hARG II**
ABH	690 nM	460 nM
1b	150.83 μM	69.50 μM
1b-1	663.93 μM	1027.27 μM
1b-2	36.65 μM	11.22 μM

[a] Mean value of triple tests.

The X-ray crystallography provides a clear understanding of the important interactions formed in the enzyme-inhibitor complexes, which is essential for this study. We investigated the X-ray crystal structures of human arginase I-**1b**, human arginase I-**1b**-1 and human arginase I-**1b**-2 determined at 1.03 Å resolution from crystals perfectly twinned by hemihedry. The conformation of the ligand inserting into the binding pocket was determined by the detected electron density. Compound **1b** is a racemic mixture of two enantiomers **1b**-1 and **1b**-2. These enantiomers could interact with human arginase I at the catalytic pocket under the tested conditions. However, we found compound **1b**-2 is the major conformation binding with human

arginase I as suggested by the X-ray crystal structure of human arginase I-**1b** (Figure 7.2). This major conformation was further confirmed by the X-ray crystal structure of human arginase I-**1b**-2 (Figure 7.3). In addition, according to the X-ray crystal structure of human arginase I-**1b**-1, clearly the boron warhead of compound **1b**-1 binds with the Mn (II) center at the active site of human arginase I. However, the interactions between the amino/tetrazolyl groups of compound **1b**-1 and the amino acid residues at the mouth site of the catalytic pocket of human arginase I cannot be determined exactly due to the insufficient electron density (Figure 7.4). This could be rationalized by the fact that compound **1b**-1 fails to recognize the amino acid networks due to its unfavorable conformation, which is also confirmed by its low inhibitory potency as discussed before.

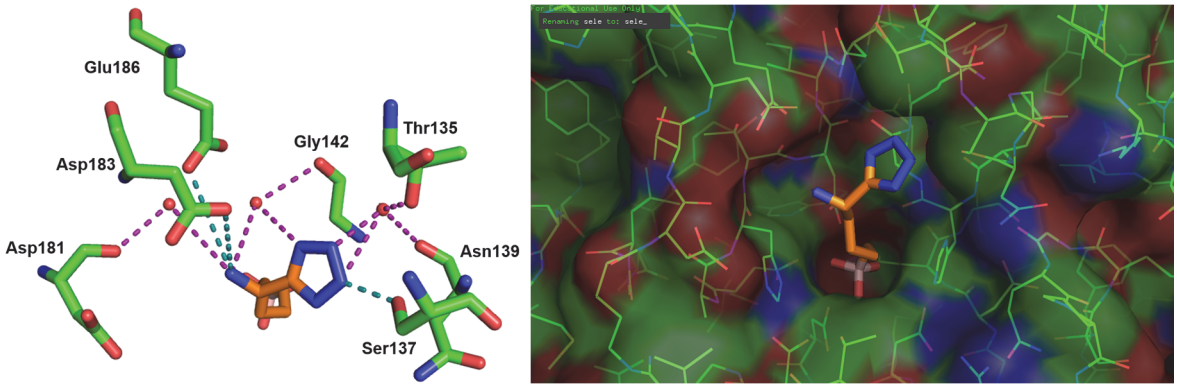

a **b**

Figure 7.2. (a) The overview of hydrogen bonding of **1b**-2 with the amino acid residues at the mouth site of human argianse I observed in the cocrystal structure of human arginase I-**1b**-2 (direct hydrogen bonds: green; water mediated hydrogen bonds: purple); and (b) the major conformation binding with human arginase I as suggested by the X-ray crystal structure of human arginase I-**1b**.

In general, the structure and activity relationship of a compound is consistent with the binding information derived from the enzyme−inhibitor complexes. Compared with ABH, a reasonable lower potency of compound **1b**-2 could be explained by the less hydrogen bond formation caused by the larger tetrazole (Table 7.6). As shown in Figure 7.3, the tetrazole substitution at α position which displaces carboxylate, results in the missing of two hydrogen bonding interactions which are observed in the crystal of human arginase I-ABH, including a direct hydrogen bonding interaction with Asn130, and a water mediated hydrogen bonding interaction with His141. The lack of these two hydrogen bonding interactions might induce a nearly 50-

fold decrease in potency with human arginase I, and a nearly 22-fold decrease with human arginase II, compared with that of ABH.

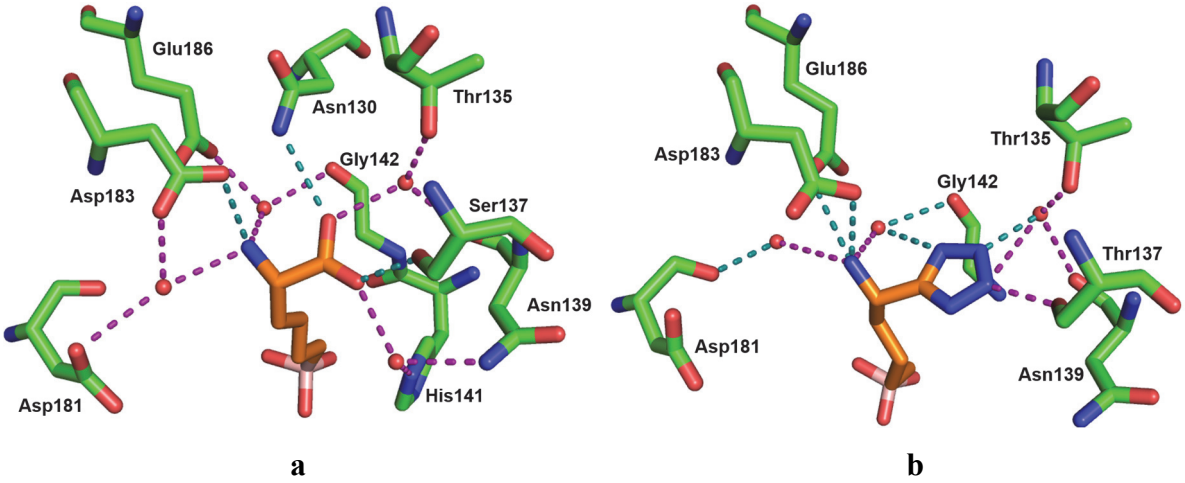

Figure 7.3. (a) (direct hydrogen bonds: green line; water mediated hydrogen bonds: purple line) The overview of hydrogen bonding of ABH with the amino acid residues at the mouth site of human argianse I (PDB: 2AEB); and (b) the overview of hydrogen bonding of compound **1b**-2 with the amino acid residues at the mouth site of human argianse I.

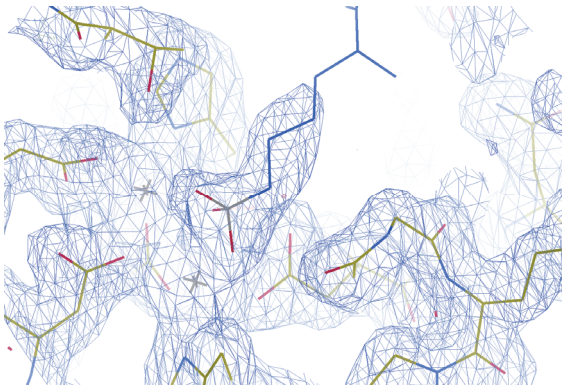

Figure 7.4. The electron density overview of the crystal structure of human argianse-**1b**-1 (blue line: **1b**-1 and yellow line: amino acid residues of human arginase I; r.m.s.d. = 1.1).

Table 7.6. The comparison of molecular properties of tetrazole and carboxylate

	Bond lengths[a]	**Topological polar surface area**
	N(1)-N(2) = 1.328 Å N(2)-N(3) = 1.333 Å N(3)-N(4) = 1.333 Å N(4)-C(7) = 1.358 Å N(1)-C(7) = 1.364 Å	54.5 Å^2 (*1H*-tetrazole)[37]

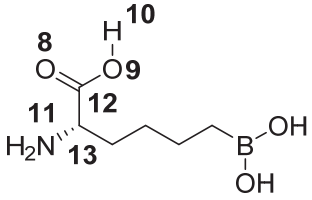	C(5)-C(7) = 1.497 Å C(5)-N(6) = 1.497 Å O(9)-H(10) = 0.972 Å O(9)-C(12) = 1.338 Å O(8)-C(12) = 1.208 Å C(12)-C(13) = 1.509 Å N(11)-C(13) = 1.468 Å	37.3 Å^2 (HCOOH)[37]

[a] Calculated using ChemBio 3D Ultra.

As shown in Figure 7.5, the X-ray crystal structure of compound **1b**-2 with human arginase I suggested that the trigonal planar boronic acid moiety, similar to that of ABH, is attacked by the metal-bridging hydroxide ion upon binding to the active site; thereby yields the tetrahedral boronate anion. The boronic acid chain of the inhibitor is buried in the active site cleft and makes contacts similar to those of ABH. The oxygen atoms linked to the boron form close contacts with the arginase Mn ions, and these substituents are surrounded by aspartic acid residues. However, compared with that of ABH, O atom of boronate which contacts with two Mn (II) ions is observed, showing a stretch away from the binuclear center (2.2 Å to 2.4 Å). Meanwhile, the distance between His141 and O atom of boronate is longer than that of ABH (2.9 Å to 3.1 Å). These prolongations on the distances between the inhibitor and the enzyme probably resulted in the insufficient lock of the active site of human arginase I which is significant to determine the catalytic activity of the enzyme. Here, we could assume that these observed insufficient interactions between the inhibitor and the active site of human arginase I probably is also due to the large size of tetrazole ring and its rigid structure.

It is interesting that compound-**1b**-2 possesses a higher inhibitory potency for human arginase II, compared with that for human arginase I (Table 7.5). Unfortunately, due to the failure of obtaining the crystal of human arginase II-**1b**-2, we could not rationalize the reason to explain this by X-ray crystallography. Although the structural biological information is missing, we could still reasonably propose that this higher inhibitory potency for human arginase II might derive from the larger volume of the human arginase II active site cleft (554 Å^3) than that of human arginase I (440 Å^3).[17] As shown in Figure 7.5, compared with human arginase I, the larger size of active site cleft of human arginase II probably benefits to form tighter interactions between compound **1b**-2 and binuclear Mn (II) center, and results more effective "locking" in the catalytic pocket.

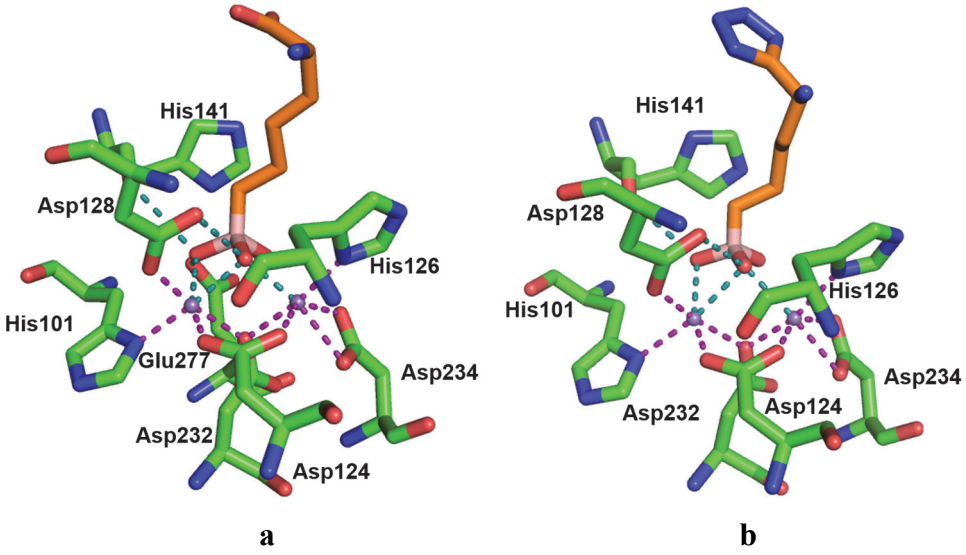

Figure 7.5. (a) Contacts of ABH with human argianse I and the Mn atoms (green line), and contacts of the Mn atoms with human argianse I (purple line) (PDB: 2AEB); and (b) contacts of compound **1b**-2 with human argianse I and the Mn atoms (green line), and contacts of the Mn atoms with human argianse I (purple line).

7.4 Conclusions

To the best of our knowledge, this is the first time that multicomponent reaction is employed to prepare novel α-isosteric tetrazole ABH analogues as promising human arginase inhibitors. However, the synthetic compounds in the *in vitro* enzyme assay showed a less potent inhibiting ability than ABH, which could be explained by the larger size of tetrazole and the less tightness of interactions between the boronate and the active site of human arginase. However, considering the higher hydrophobicity and metabolism stability of tetrazole, we could foresee that the leading compound **1b-**2, a novel α-isosteric tetrazole ABH analogue, might be more potent in the *in vivo* assay and clinical studies. Besides, the structure of tetrazole ABH analogues can be optimized, to achieve higher inhibitory potency. The relevant research is ongoing in our lab.

7.5 Experimental section

7.5.1 General procedure

Nuclear magnetic resonance spectra were recorded on a Bruker Avance 500 spectrometer (^{1}H NMR (500 MHz), ^{13}C NMR (126 MHz)) or a Varian Inova 400 MHz spectrometer (^{1}H NMR (400 MHz), ^{13}C NMR (100 MHz)) or a Varian VXR 300 MHz spectrometer (^{1}H NMR (300 MHz), ^{13}C NMR (75 MHz)). Chemical shifts for ^{1}H NMR were reported as δ values and

coupling constants were in hertz (Hz). The following abbreviations were used for spin multiplicity: s = singlet, d = doublet, t = triplet, dd = double doublet, m = multiplet. Chemical shifts for ^{13}C NMR reported in ppm relative to the solvent peak. Mass spectra (HRMS) were recorded on an Orbitrap XL (Thermo Fisher Scientific; ESI pos. mode, resolution of 60000@m/z 400). Electrospray ionization mass spectra (ESI-MS) were recorded on a Waters Investigator Semi-prep 15 SFC-MS instrument. Mass spectra for deprotected α-amino acid-isosteric α-amino tetrazoles were measured on an API 3000 triple-quadrupole mass spectrometer (Applied Biosystems/MDS Sciex) via a TurboIon Spray source. Thin layer chromatography was performed on precoated silica gel plates (TLC Silica gel 60 F_{254}). Flash chromatography was performed on a Teledyne ISCO Combiflash R_f, using RediSep R_f Normal-phase Silica Flash Columns (Silica Gel 60 Å, 230 - 400 mesh). Reagents were available from commercial suppliers and used without any purification unless otherwise noted. All reaction solvents were of chemical grade. All eluted phases were of HPLC grade for chiral separation.

7.5.1.1 Synthesis of 5-(4,4,5,5-tetramethyl-1,3,2-dioxaborolan-2-yl)pentanal

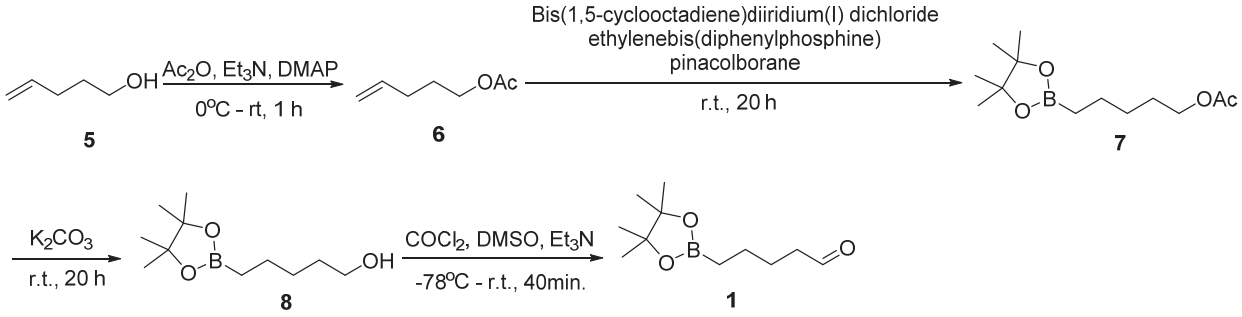

Pent-4-en-1-yl acetate (6)

To a solution of 1-Pentenol (20 g, 232 mmol) in 100 mL CH_2Cl_2 was added Et_3N (65mL, 464 mmol) and DMAP (0.68 g, 5.5 mmol). The mixture was cooled to 0°C using an ice bath and acetic anhydride (25mL, 255 mmol) was added drop wise. The mixture was stirred at RT for 1 hour. The mixture was diluted using 100 mL CH_2Cl_2 and washed with water (2×100 mL), 1M HCl (3×20 mL), brine (3×20mL). The organic layer was collected and dried over $MgSO_4$, filtered and concentrated under reduced pressure to obtain the product 27 gram (90%) as a colorless oil. ^1H NMR (400 MHz, Chloroform-*d*) δ 5.83 – 5.78 (m, 1H), 5.06 – 4.90 (m, 2H), 4.07 (t, *J* = 6.7, 2H), 2.15 – 2.10 (m, 2H), 2.04 (d, *J* = 3.2 Hz, 3H), 1.76 – 1.70 (m, 2H). ^{13}C NMR (126 MHz, $CDCl_3$) δ 171.1, 137.6, 115.4, 64.0, 30.1, 28.0, 21.0 ppm.

5-(4,4,5,5-tetramethyl-1,3,2-dioxaborolan-2-yl)pentyl acetate (7)

To a solution of the Iridium catalyst (395 mg, 0.6 mmol) and ethylenebis(diphenylphosphine) (492 mg, 1.2 mmol) in 50 mL was added the alkene **2** (5.5 g, 43 mmol) and pinacolborane (6,0 g, 47 mmol). The mixture was stirred for 20 hours and then quenched using 10 mL MeOH, washed with water (2×50 mL), brine (3×20 mL), dried over $MgSO_4$, filtered and concentrated under reduced pressure to obtain the crude product 11.5 gram crude product as a yellow oil. The crude product was purified by flash chromatography (Combiflash) yielding 7.8 g (83%) of **3** as a colorless oil. ^{1}H NMR (500 MHz, Chloroform-*d*) δ ^{1}H NMR (500 MHz, $CDCl_3$) δ 4.06 (t, *J* = 6.8, 2H), 2.07 – 2.01 (m, 3H), 1.68 – 1.59 (m, 2H), 1.48 – 1.42 (m, 2H), 1.39 – 1.35 (m, 2H), 1.26 – 1.25 (s, 12H), 0.79 (t, *J* = 7.7, 2H) ppm; ^{13}C NMR (126 MHz, $CDCl_3$) δ 83.1, 64.8, 28.7, 28.6, 25.0, 24.7, 23.8, 21.1 ppm.

5-(4, 4, 5, 5-tetramethyl-1, 3, 2-dioxaborolan-2-yl)pentan-1-ol (8)

To a solution of the acetyl ester **3** (11 g, 43 mmol) in 150 mL EtOH was added K_2CO_3 (11.3 g, 82 mmol). After 20 hours of stirring at r.t., the solvent was removed under reduced pressure. The resultant mixtue was redissolved in 100 mL EtOAc, washed with water (3×100 mL), brine (3×20 mL), dried over $MgSO_4$, filtered and concentrated under reduced pressure to obtain 13 gram crude product. Further purification was performed by flash chromatography to obtain 6.7 g (77%) of **4** as a slightly yellow oil. ^{1}H NMR (500 MHz, Chloroform-*d*) δ 3.62 (t, *J* = 6.6, 1H), 1.59 – 1.54 (m, 2H), 1.46 – 1.41 (m, 2H), 1.39 – 1.34 (m, 2H) 1.25 (s, 12H), 0.79 (t, *J* = 7.6 Hz, 2H) ppm; ^{13}C NMR (101 MHz, Chloroform-*d*) δ 83.1, 64.7, 28.7, 28.5, 24.9, 24.7, 23.8, 21.1 ppm.

5-(4, 4, 5, 5-tetramethyl-1, 3, 2-dioxaborolan-2-yl)pentanal (1)

Oxalyl chloride (3.2 mL, 38 mmol) was dissolved in CH_2Cl_2 and cooled to -78°C. DMSO (8.9 mL, 125 mmol) was dissolved in 9 mL and drop wise added. After 15 minutes of stirring, the alcohol **4** (6.7 g, 31 mmol) was dissolved in 7 mL CH_2Cl_2 and drop wise added to the reaction mixture and stirred for 40 minutes. Et_3N (26.2 mL, 188 mmol) was drop wise added and the mixture was left to warm to room temperature. The mixture was diluted with 100 mL CH_2Cl_2 and poured onto 100 mL ice-water. The mixture was washed with water (2×50 mL), brine (3×20 mL), dried over $MgSO_4$, filtered and concentrated under reduced pressure to obtain 12 gram crude product. The title compound **5** was afforded by flash chromatography purification yielding 4.6 g (69%) as a slightly yellow oil. ^{1}H NMR (500 MHz, Chloroform-*d*)

δ 9.76 – 9.75 (m, 1H), 2.44 – 2.40 (m, 2H), 1.68 – 1.61 (m, 2H), 1.50 – 1.43 (m, 2H), 1.25 (d, *J* = 3.1 Hz, 12H), 0.82 – 0.78 (m, 2H) ppm; ^{13}C NMR (75 MHz, Chloroform-*d*) δ 203.1, 83.1, 83.0, 43.9, 24.9, 24.8, 24.7, 23.8 ppm.

7.5.1.2 Synthesis of *tert*-octyl isocyanide (3)

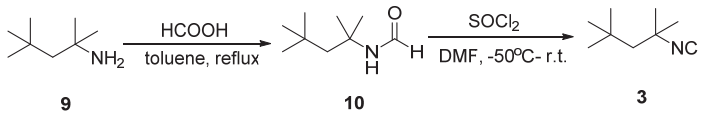

9 10 3

N-(2, 4, 4-trimethylpentan-2-yl)formamide (10)

A solution of *tert*-octylamine (250 ml, 1.56 mol) and 98 % formic acid (138 ml, 3.58 mol) in toluene (400 ml) is refluxed under a condenser. After the reaction was complete, volatile materials were removed by evaporation. *N*-(2, 4, 4-trimethylpentan-2-yl)formamide was obtained as a colorless oil (235 g, 96%). ^{1}H NMR (500 MHz, Chloroform-*d*) δ 1.75 (d, *J* = 4.4 Hz, 1H), 1.56 (d, *J* = 4.4 Hz, 1H), 1.44 (d, *J* = 4.5 Hz, 3H), 1.39 (d, *J* = 4.5 Hz, 4H), 1.02 (d, *J* = 4.0 Hz, 9H) ppm.

2-isocyano-2, 4, 4-trimethylpentane (3)

In a 3L three necked round bottomed flask fitted with a mechanic stirrer, a 500ml pressure equalizing addition funnel, and nitrogen-inlet tube is flamed fry under a nitrogen atmosphere and allowed to cool. The nitrogen-inlet tube is replaced with a low temperature thermometer, and the nitrogen line was attached to a Y tune placed on the addition funnel. To the flask are added 40 g of amide and 500 ml DMF. The addition funnel is charged with a premixed solution of 19 ml of thionyl chloride and 78 ml DMF. The flask is immersed in an acetone- liquid nitrogen and moderately fast stirring is started. When reaction temperature reaches to -50^{o}C, the solution in the funnel is added at a rate to keep the temperature between -55 to -50^{o}C. After addition is complete, the bath was removed to allow the temperature to -35^{o}C, the bath was replaced, 50g Na_2CO_3 was added. Then the reaction mixture continued to stir for 6h at r.t.

The reaction mixture was poured into a flask with 1 L ice and water. The residue in the reaction flask was dissolved in water and 300ml petrol ether was added. The organic phase was separated and washed with water for 2 times, dried over MgSO4, filtered, and concentrated.

The crude product was distilled under reduced pressure and collected the fractions at 135-145^{o}C under membrane pump to yield the product as a colorless oil (24 g, 67%). ^{1}HNMR: (500

MHz, $CDCl_3$) δ 1.62 – 1.58 (m, 2H), 1.51 – 1.45 (m, 6H), 1.08 (s, 9H) ppm; ^{13}C NMR (126 MHz, $CDCl_3$) δ 154.6, 56.9, 53.8, 31.9, 31.6, 31.0 ppm.

7.5.1.3 General procedure for the synthesis of Ugi products (1a – 13a)

Aldehyde (1 mmol) and amine (1 mmol) were suspended in MeOH (1 mL) in a sealed vial with a magnetic stirring bar. The reaction stirred for 5 minutes at room temperature. Then isocyanide (1 mmol) and azidotrimethylsilane (1 mmol) were added into the reaction mixture and further stirred for 24h at room temperature. The solvent was removed under reduced pressure and the residue was purified using flash chromatography to obtain the target product.

7.5.1.4 General procedure for the synthesis of α-isosteric tetrazole ABH analogue (1b – 3b)

The Ugi products (**1a** – **3a**) was dissolved in 6 N HCl and refluxed for 24 h. The reaction mixture were purified by silica column or cation exchange chromatography purification yielding α-isosteric tetrazole ABH analogues (**1b** – **3b**).

7.5.1.5 General procedure for the synthesis of α-isosteric tetrazole ABH analogue (4b – 9b)

To a solution of Ugi product (**4a** – **9a**, 1 mmol) in acetone (0.08 mmol /1mL) and H_2O (0.08 mmol /0.5 mL) were added $NaIO_4$ (3 mmol) and NH_4OAc (3 mmol). The suspension was stirred at room temperature for 3 days. The reaction mixture was dissolved into water and extracted with EtOAc. The organic phase was seperated and washed with water, brine, dried over $MgSO_4$, filtrated, concentrated in vacuum. The purification was carried by silica gel flash column chromatography yielding α-isosteric tetrazole ABH analogues (**4b** – **9b**).

7.5.1.6 General procedure for the synthesis of α-isosteric tetrazole ABH analogue (10b – 13b)

The Ugi products (**10a** – **13a**, 1 mmol) was dissolved in a mixture of acetone (0.08 mmol /1mL) and H_2O (0.08 mmol /0.5 mL) with $NaIO_4$ (3 mmol) and NH_4OAc (3 mmol). The reaction mixture stirred for 3 days at room temperature. The reaction mixture was extracted with EtOAc (50 mL×3), and then the organic phases were combined, concentrated. The residue were redissoved in TFA and stirred for 1 min at room temperature. The reaction mixture were purified by flash chromatagraphy yielding α-isosteric tetrazole ABH analogues (**10b** – **13b**).

5-(4, 4, 5, 5-tetramethyl-1, 3, 2-dioxaborolan-2-yl)-1-(1-(2, 4, 4-trimethylpentan-2-yl)-1H-tetrazol-5-yl)-*N*-tritylpentan-1-amine (1a)

^{1}H NMR (500 MHz, Chloroform-*d*) δ 7.45 – 7.43 (m, 6H), 7.21 – 7.18 (m, 6H), 7.15 – 7.12 (m, 3H), 4.30 – 4.27 (m, 1H), 1.71 (d, *J* = 5.9 Hz, 2H), 1.50 (s, 4H), 1.41 (s, 4H), 1.35 – 1.29 (m, 2H), 1.21 (d, *J* = 1.7 Hz, 12H), 1.16 – 1.08 (m, 1H), 0.80 (s, 9H), 0.70 (t, *J* = 7.7 Hz, 2H) ppm; ^{13}C NMR (126 MHz, Chloroform-*d*) δ 157.6, 146.1, 129.0, 127.9, 126.6, 83.0, 71.8, 65.8, 55.3, 49.8, 37.3, 31.6, 31.2, 30.1, 28.6, 26.8, 24.9, 24.9 ppm.

***tert*-butyl 2-(5-(4,4,5,5-tetramethyl-1,3,2-dioxaborolan-2-yl)-1-(1-(2,4,4-trimethylpentan-2-yl)-1H-tetrazol-5-yl)pentyl)hydrazine-1-carboxylate (2a)**

^{1}H NMR (500 MHz, Chloroform-*d*) δ 4.67 (dd, *J* = 8.4, 4.9 Hz, 1H), 1.97 (s, 2H), 1.83 (d, *J* = 11.8 Hz, 6H), 1.66 – 1.55 (m, 1H), 1.53 – 1.41 (m, 3H), 1.41 (s, 9H), 1.22 (s, 12H), 0.82 (s, 9H), 0.78 – 0.76 (m, 2H) ppm; ^{13}C NMR (126 MHz, Chloroform-*d*) δ 156.5, 156.4, 83.0, 80.7, 65.2, 56.8, 54.2, 33.6, 31.7, 30.8, 30.7, 30.3, 30.0, 28.8, 28.4, 24.9, 24.0 ppm.

***tert*-butyl 2-methyl-1-(5-(4,4,5,5-tetramethyl-1,3,2-dioxaborolan-2-yl)-1-(1-(2,4,4-trimethylpentan-2-yl)-1H-tetrazol-5-yl)pentyl)hydrazine-1-carboxylate (3a)**

^{1}H NMR (500 MHz, Chloroform-*d*) δ 4.97 (s, 1H), 4.71 (s, 1H), 2.82 (s, 3H), 2.09 (s, 1H), 1.95 (dd, *J* = 18.4, 6.8, 3H), 1.85 (d, *J* = 5.9, 4H), 1.82 (d, *J* = 12.2, 7H), 1.51 – 1.39 (m, 12H), 1.28 – 1.18 (m, 14H), 0.83 (s, 9H), 0.80 – 0.74 (m, 8H); ^{13}C NMR (126 MHz, Chloroform-*d*) δ 156.3, 140.7, 82.8, 81.0, 65.0, 62.7, 55.4, 54.2, 54.1, 33.7, 31.5, 31.4, 30.7, 30.5, 30.5, 30.2, 29.81, 28.9, 28.2, 24.7, 23.9, 10.8 ppm.

(5-amino-5-(1H-tetrazol-5-yl)pentyl)boronic acid (1b)

^{1}H NMR (300 MHz, Deuterium Oxide) δ 4.74 (t, *J* = 7.4 Hz, 1H), 2.14 – 2.06 (m, 2H), 1.46 – 1.55 (m, 2H), 1.33 – 1.14 (m, 2H), 0.70 (t, *J* = 7.7 Hz, 2H) ppm; ^{13}C NMR (126 MHz, methanol-d_4) δ 162.1, 36.0, 35.9, 30.5, 26.0 ppm.

(5-hydrazinyl-5-(1H-tetrazol-5-yl)pentyl)boronic acid (2b)

^{1}H NMR (500 MHz, methanol-d_4) δ 4.19 (s, 1H), 1.55 (d, *J* = 28.8, 2H), 1.11 – 0.78 (m, 4H), 0.35 (t, *J* = 6.7, 2H) ppm; ^{13}C NMR (126 MHz, methanol-d_4) δ 158.7, 55.8, 55.7, 49.7, 49.5, 49.3, 49.2, 49.0, 48.8, 48.6, 33.4, 29.0, 24.6 ppm.

(5-(2-methylhydrazinyl)-5-(1H-tetrazol-5-yl)pentyl)boronic acid (3b)

^{1}H NMR (500 MHz, methanol-d_4) δ 4.44 (t, J = 6.6 Hz, 1H), 2.58 (d, J = 24.2 Hz, 3H), 1.79 – 1.56 (m, 2H), 1.19 – 0.85 (m, 4H), 0.47 (t, J = 7.4 Hz, 2H) ppm; ^{13}C NMR (126 MHz, methanol-d_4) δ 158.7, 54.5, 49.7, 49.5, 49.3, 49.2, 49.0, 48.8, 48.6, 36.3, 36.2, 33.7, 29.0, 24.6 ppm.

(5-(4-methylpiperazin-1-yl)-5-(1H-tetrazol-5-yl)pentyl)boronic acid (4b)

^{1}H NMR (400 MHz, methanol-d_4) δ 4.30 – 4.19 (m, 1H), 3.49 (s, 2H), 3.16 (s, 3H), 2.87 (s, 3H), 2.73 – 2.38 (m, 2H), 2.12 – 1.90 (m, 2H), 1.49 – 1.12 (m, 4H), 0.75 (d, J = 6.6, 2H)ppm; ^{13}C NMR (101 MHz, methanol-d_4) δ 156.81, 59.74, 54.98, 43.69, 31.19, 29.93, 24.64 ppm.

(5-(benzyl(methyl)amino)-5-(1H-tetrazol-5-yl)pentyl)boronic acid (5b)

^{1}H NMR (500 MHz, methanol-d_4) δ 4.24 (dd, J = 9.9, 4.3, 1H), 2.75 - 2.67 (m, 2H), 2.48 - 2.40 (m, 2H), 2.30 - 2.20 (m, 1H), 2.19 (dd, J = 21.1, 10.1, 1H), 1.99 (d, J = 15.1, 1H), 1.95 - 1.86 (m, 4H), 1.83 (s, 3H), 1.66 (s, 1H), 1.53 - 1.35 (m, 5H), 1.35 - 1.07 (m, 20H), 0.84 (s, 9H), 0.80 (t, J = 7.3, 7H), 0.76 (t, J = 7.8, 2H) ppm; ^{13}C NMR (50 MHz, methanol-d_4) δ 157.4, 132.5, 131.3, 130.5, 130.4, 60.3, 50.4, 47.9, 29.9, 29.2, 24.3 ppm.

(5-(4-benzylpiperidin-1-yl)-5-(1H-tetrazol-5-yl)pentyl)boronic acid (6b)

^{1}H NMR (500 MHz, methanol-d_4) δ 7.22 (t, J = 7.9 Hz, 1H), 7.03 (d, J = 8.3 Hz, 1H), 6.94 (t, J = 7.3 Hz, 0H), 3.41 (d, J = 58.0 Hz, 3H), 3.24 (s, 1H), 3.22 – 3.16 (m, 0H), 2.36 – 2.16 (m, 1H), 1.30 (ddd, J = 22.1, 14.6, 7.5 Hz, 1H), 1.17 (dt, J = 14.0, 6.2 Hz, 0H), 0.95 (dt, J = 12.9, 6.6 Hz, 0H), 0.69 – 0.53 (m, 1H); ^{13}C NMR (50 MHz, methanol-d_4) δ 158.0, 149.3, 130.7, 124.5, 119.1, 62.1, 49.5, 30.1, 29.3, 24.5 ppm.

(5-(di(prop-2-yn-1-yl)amino)-5-(1H-tetrazol-5-yl)pentyl)boronic acid (7b)

^{1}H NMR (500 MHz, methanol-d_4) δ 4.24 (dd, J = 9.9, 4.3, 1H), 2.75 - 2.67 (m, 2H), 2.48 - 2.40 (m, 2H), 2.30 - 2.20 (m, 1H), 2.19 (dd, J = 21.1, 10.1, 1H), 1.99 (d, J = 15.1, 1H), 1.95 - 1.86 (m, 4H), 1.83 (s, 3H), 1.66 (s, 1H), 1.53 - 1.35 (m, 5H), 1.35 - 1.07 (m, 20H), 0.84 (s, 9H), 0.80 (t, J = 7.3, 7H), 0.76 (t, J = 7.8, 2H) ppm; ^{13}C NMR (50 MHz, methanol-d_4) δ 157.4, 132.5, 131.3, 130.5, 130.4, 60.3, 50.4, 47.9, 29.9, 29.2, 24.3 ppm.

(5-(4-benzylpiperidin-1-yl)-5-(1H-tetrazol-5-yl)pentyl)boronic acid (8b)

^{1}H NMR (500 MHz, methanol-d_4) δ 4.24 (dd, J = 9.9, 4.3, 1H), 2.75-2.67 (m, 2H), 2.48-2.40 (m, 2H), 2.30-2.20 (m, 1H), 2.19 (dd, J = 21.1, 10.1, 1H), 1.99 (d, J = 15.1, 1H), 1.95 - 1.86 (m, 4H), 1.83 (s, 3H), 1.66 (s, 1H), 1.53 - 1.35 (m, 5H), 1.35 - 1.07 (m, 20H), 0.84 (s, 9H), 0.80 (t, J = 7.3, 7H), 0.76 (t, J = 7.8, 2H) ppm; ^{13}C NMR (50 MHz, methanol-d_4) δ 157.1, 140.5, 130.3, 129.6, 127.4, 63.2, 53.3, 42.8, 36.6, 30.7, 30.3, 29.8, 24.5 ppm.

(5-(methyl(prop-2-yn-1-yl)amino)-5-(1H-tetrazol-5-yl)pentyl)boronic acid (9b)

^{1}H NMR (500 MHz, methanol-d_4) δ 5.02 – 4.95 (m, 1H), 4.02 (dd, J = 41.9, 16.6, 2H), 3.19 (s, 1H), 2.86 (s, 3H), 2.25 (d, J = 9.2, 1H), 2.11 (s, 1H), 1.40 – 1.19 (m, 2H), 1.13 (s, 1H), 0.94 (s, 1H), 0.61 (s, 2H) ppm; ^{13}C NMR (50 MHz, methanol-d_4) δ 157.8, 81.7, 73.1, 60.6, 45.3, 38.1, 30.2, 29.2, 24.4 ppm.

(5-amino-5-(1-(2-((4-chlorobenzyl)amino)-2-oxoethyl)-1H-tetrazol-5-yl)pentyl)boronic acid (10b)

^{1}H NMR (400 MHz, methanol-d_4) δ 7.31 – 7.22 (m, 4H), 5.41 (d, J = 5.2, 2H), 4.38 (d, J = 2.1, 2H), 3.29 – 3.24 (m, 1H), 2.25 – 1.97 (m, 2H), 1.43 – 1.17 (m, 4H), 0.73 (s, 2H) ppm; ^{13}C NMR (50 MHz, methanol-d_4) δ 166.9, 155.4, 138.0, 136.4, 134.4, 130.5, 129.8, 50.5, 45.9, 44.0, 33.3, 28.6, 24.5 ppm.

(5-amino-5-(1-(2-morpholinoethyl)-1H-tetrazol-5-yl)pentyl)boronic acid (11b)

^{1}H NMR (400 MHz, methanol-d_4) δ 4.98 (t, J = 7.1, 2H), 3.86 (s, 4H), 3.61 (s, 2H), 3.30 (dt, J = 3.2, 1.6, 2H), 3.20 (s, 4H), 2.10 (dd, J = 14.0, 7.0, 2H), 1.42 (d, J = 4.7, 3H), 1.25 (dd, J = 16.7, 9.5, 1H), 0.75 (d, J = 33.2, 2H) ppm; ^{13}C NMR (50 MHz, methanol-d_4) δ 154.8, 66.0, 56.9, 54.2, 50.4, 50.0, 49.6, 49.2, 48.7, 48.3, 47.9, 46.0, 44.2, 34.1, 28.6, 24.7 ppm.

(5-amino-5-(1-(2-oxo-2-(4-phenylpiperazin-1-yl)ethyl)-1H-tetrazol-5-yl)pentyl)boronic acid (12b)

^{1}H NMR (400 MHz, methanol-d_4) δ 7.19 (tt, J = 4.2, 2.1, 2H), 6.94 (dd, J = 8.7, 0.9, 2H), 6.81 (dd, J = 10.4, 4.1, 1H), 5.72 (dd, J = 37.9, 17.2, 2H), 4.74 (t, J = 7.1, 1H), 3.70 (d, J = 4.4, 4H), 3.27 – 3.18 (m, 2H), 3.17 – 3.07 (m, 2H), 2.28 – 1.88 (m, 2H), 1.46 – 1.11 (m, 4H), 0.67 (d, J = 12.6, 2H) ppm; ^{13}C NMR (50 MHz, methanol-d_4) δ 165.2, 155.8, 152.5, 130.3, 121.9, 118.2, 50.9, 50.5, 50.4, 49.8, 46.2, 45.9, 43.7, 33.5, 30.8, 28.6, 24.6 ppm.

(5-amino-5-(1-(4-methoxy-2-nitrophenyl)-1H-tetrazol-5-yl)pentyl)boronic acid (13b)

^{1}H NMR (500 MHz, methanol-d_4) δ 7.92 (s, 1H), 7.79 (d, J = 8.9 Hz, 1H), 7.56 (d, J = 8.8 Hz, 1H), 4.04 (d, J = 3.5 Hz, 3H), 2.01 – 1.89 (m, 2H), 1.32 – 1.21 (m, 4H), 0.68 – 0.60 (m, 2H) ppm; ^{13}C NMR (50 MHz, methanol-d_4) δ 164.2, 155.7, 147.0, 132.0, 121.2, 118.9, 113.6, 113.6, 57.5, 46.6, 33.5, 27.9, 24.3 ppm.

7.5.2 Chiral separation

The chiral separation of compound **1a** (racemic mixture) was performed at 40ºC on a supercritical fluid chromatography system (SFC, Waters), using a chiral column CHIRALPAK®IC (10×250 mm, Daicel Corporation). The eluents were CO_2 and isopropanol, with a flow rate of 15 mL/min.

7.5.3 Optical rotation analysis

The polarimeters of enantiormers **1a**-1 and **1a**-2, as well as, enantiomers **1b**-1 and **1b**-2, were tested on a Schmidt+ Haensch polarimeter (Polartronic MH8) with a 10 cm cell. The obtained α_D^{20} values were -17.4 (C = 1.01, $CHCl_3$), +16.7 (C = 1.04, $CHCl_3$), -0.028 (C = 0.218, H_2O), +0.033 (C = 0.15, H_2O), respectively.

7.5.4 Enzymatic assays

Arginase converts L-arginine to L-ornithine and urea. The relative arginase activity was determined by measuring urea levels in a colorimetric assay according to methods reported in literature.[30, 35] Lab-made, purified recombinant full length human arginase I protein and commercially available recombinant, fully active, truncated form of human arginase II were used to develop 96-well plate human arginase I and arginase II assays. Inhibition of arginase I and arginase II by program compounds was followed spectrophotometrically at 530 nm. The assay buffer was 0.1 M sodium phosphate buffer containing 130 mM NaCl and 1 mg/ml ovalbumin (OVA) at a pH of 7.4. The tested compound was dissolved in ultrapure water (UP) at an initial concentration of 100 mM, used as the stock solution. Then different concentrations of the tested compounds were diluted with assay buffer, and used as the test compound solutions at the concentrations of 1, 10, 100, 1000, 10000 μm for **1b**, **1b**-1, **1b**-2, and 0.1, 1, 10, 100, 1000 μM for the reference compound ABH. Solutions of human arginase I and II were prepared in assay buffer to give an arginase stock solution at a final concentration of 1.28 μg/mL and 1.0 ug/ml, respectively. The enzyme substrate solution was prepared by dissolving L-arginine,

glycine and manganese chloride in UP, with the final concentration of 49.8 mM, 82.8 mM and 1.8 mM, respectively. To each tested compounds, the well of a 96-well microtiter plate was added with 40 µL of enzyme (1.28 µg/ ml for hArg I and 1.0 µg/ ml for hArg II in the assay buffer), 10 µL of the tested compound solution. After pre-incubating the microtiter plate at 37°C for 30 min, 10 µL of the enzyme substrate solution was added to each well referred above. For wells that were used as positive controls, only the enzyme and substrate buffer were added, while wells used as negative controls contained only manganese chloride. The microtiter plate was incubated at 37 °C for 60 min again. After the completion of the second incubation, 150 µL of a urea reagent obtained by combining equal proportions (1:1) of reagents A and B was added to each well of the microtiter plate to stop the reaction. The urea reagent was made just before use by combining Reagent A (10 mM o-phthaldialdehyde and 0.4% polyoxyethylene lauryl ether (w/v) in 1.8 M sulfuric acid) with Reagent B (1.3 mM primaquine diphosphate, 0.4% polyoxyethylene lauryl ether (w/v), and 130 mM boric acid in 3.6 M sulfuric acid). After quenching the reaction mixture, the microtiter plate was allowed to stand for an additional 10 min at room temperature for color development. The inhibition of arginase was computed by measuring the optical density (OD) of the reaction mixture at 530 nm and normalizing the OD value to the percent of inhibition observed in the control. The normalized OD was then used to generate a concentration-response curve by plotting the normalized OD values against log[concentration] and using Prism to compute the IC_{50} values.

7.5.5 Purification and X-ray crystallization of human arginase I with ATPBA

7.5.5.1 Cloning of arginase I

The gene of *H. sapiens* arginase I was amplified by polymerase chain reaction (PCR) using sequence-specific sense (5'-GGCGGC**TCATGA**GCGCCAAGTCCAGAACCATA-3') and antisense (5'-GCCGCC**AAGCTT**ACTTAGGTGGGTTAAGGTAGTCAATA-3') oligonucleotides containing BspHI and HindIII restriction sites (indicated in bold) and pANT7_cGST_ARGI (http://dnasu.org/DNASU/GetCloneDetail.do?cloneid=616540) plasmid as a template. The PCR was performed with Phusion HF polymerase (Thermo scientific) using the following conditions: one cycle of 371 K for 30 seconds followed by 35 cycles of 5 seconds at 371 K, 30 seconds at 331 K and 30 sec at 345 K, followed by one cycle of 345 K for 10 min. The PCR fragments were cloned into petM11 vector (https://www.embl.de/pepcore/pepcore_services/cloning/pdf/pETM-11.pdf) previously digested with NcoI and HindIII. The ligation was performed using T4 DNA ligase for 10 min

at 295 K followed by heat inactivation at 338 K for 10 min according to the manufacturer's recommendations (Thermo Scientific). The final construct consisted of full-length Arginase I with the additional amino acids HHHHHHHLKR (6-His-tag with TEV protease restriction site) at the N-terminus.

7.5.5.2 Expression of human arginase I

Human arginase I was recombinantly expressed in *E. coli* BL21 (DE3) RIL cells (Novagen) using the expression plasmid pETM11-ArgI, which contains the open reading frame for the hArg I gene fused to a N-terminal TEV-cleavable His tag to facilitate purification. Transformed *E. coli* BL21 (DE3) RIL cells were propagated in 0.5 L of selective autoinducing medium (ZYM5052) in the presence of 100 µg/mL Kanamycin, 35 µg/mL Chloramphenicol) at overnight at 310 K in 2 L baffled Erlenmeyer flasks (Nalgene, US) according to the autoinduction protocol.[38] After the culture reached an OD_{600} of approx. 2.0 the temperature of the culture was lowered to 291 K and the cells were harvested by centrifugation (5000 rev min^{-1} for 30 min) after an overnight expression.

7.5.5.3 Purification of human arginase I

The bacteria pellet was resuspended in 30 ml Lysis buffer *A* [50 mM Tris pH 8.0, 300 mM NaCl, 20 mM imidazole, 5% (v/v) glycerol, 3 mM β-mercaptoethanol (BME)]. The cells were lysed on ice by sonication and the homogenate was clarified by centrifugation at 19000 rev $min^{-1}$for 60 min.

The supernatant containing the soluble His-tagged protein was filtered using 0.45 µm filter (Whatman) and incubated for 20 min with 2 ml Ni-NTA Agarose (Protino, Macherey Nagel) at room temperature. The Ni-NTA resin was further collected by pouring the mixture into a gravity-flow column (Bio-Rad) and washed with 50 - 100 ml of buffer *A*. The protein was eluted with 10 ml of Elution buffer E [50 mM Tris pH 8.0, 300 mM NaCl, 250 mM imidazole, 5% (v/v) glycerol, 3 mM BME].

The elution fraction was mixed with 1.5 mg of recombinant TEV protease and dialysed overnight at 277 K against 0.5 L of buffer A to remove the excess of Imidazole. Digested sample was further incubated for 10 min with 1.5 ml Ni-NTA Agarose (Macherey Nagel) at room temperature to remove the undigested material, cleaved His-tag and His-tagged TEV protease. The Ni-agarose beads were poured into a gravity-flow column (Bio-Rad) and the flow through was collected and concentrated to a maximum concentration of 10 mg ml^{-1} and purified via

size-exclusion chromatography (SEC) using HiLoad 16/60 Superdex 75 column (GE Healthcare) equilibrated with SEC buffer (10 mM Ammonium acetate pH 7.3, 150 mM NaCl, 2 mM MnCl, 5% v/v Glycerol, 2 mM BME) and automated NGC chromatography system (BioRad). The SEC buffer was chosen based upon a Thermofluor-based stability assay.[39, 40]

Thermofluor data were collected on a CFX96 Real-Time PCR System (BioRad). SYPRO Orange fluorescent dye (Invitrogen) was added to the protein sample (concentrated to 0.5 mg mL^{-1}) at 1:500 dilution. Experiments were composed of 5µL of protein/dye solution and 45 µL of buffer component to be screened. Inflection points in graphs of relative fluorescence units (RFU) against temperature were determined manually and used as an indicator of the sample thermal stability in the buffer component screened. Comparisons were made against control samples containing only protein/water mixture. The optimal buffer composition was 10 mM ammonium acetate pH 7.3, 150 mM NaCl, 2 mM MnCl, 5% v/v Glycerol, 2 mM BME.

The final purified protein eluted as a single peak. This peak was pooled and concentrated using a centrifuge concentration unit with a 10 kDa cutoff (Sartorius).

The final protein concentration was determined to be 10 mg mL^{-1} based upon its theoretical absorbance at 280 nm [$Abs_{0.1\%}$(1 mg ml^{-1}) = 0.68; http://web.expasy.org/protparam/]. The final yield of purified hArg I was approximately 40 mg per liter of bacterial culture. The protein was concentrated and immediately used in crystallization trials. The protein purity was estimated to be better than 95% using Coomassie Brilliant Blue-stained SDS-PAGE.[41]

7.5.6 Crystallization

An initial screening was performed via the sitting drop vapour diffusion technique using Pact Premier and JCSG + sparse matrix screens (Molecular Dimensions) and MRC2 96-well plates using high-throughput crystallization robot Gryphon (Art Robbins Instruments). The final concentration of the protein was 10 mg mL^{-1}. The drops of 0.3 – 0.2 µL consisted of 2:1 or equal amounts of the protein and the crystallization liqueur, respectively. The plates were sealed and stored at controlled temperature (288 K). Initial diffraction quality crystals appeared after several months in 0.1 M MIB buffer (Maleic acid, Imidazole, Boric acid) pH 6.0 and 25 % (w/v) PEG 1500 (Condition B3, PACT *Premiere*, Molecular Dimensions Ltd.). Based on the result of the screening manual optimization was performed. The purified hArg I at the concentration of 10 mg mL^{-1} was mixed with 10 mM of the compound of choice (**1b**, **1b**-1 or **1b**-2) diluted in water and 10% of the B3 PACT condition prior the crystallization. Optimized

diffraction quality crystals appeared overnight in 24-well hanging drop crystallization plates in 0.1 M MIB buffer pH 6-9 and 25-27% PEG 2000.

These crystals were briefly soaked in the cryo-protection buffer and flash-frozen in liquid nitrogen for further storage and shipment to the synchrotron. The Cryo buffer was chosen based on the initial estimation from [42] and consisted of 20% (v/v) glycerol and 10 mM of the compound of choice in addition to the crystallization liquor composition. Interestingly, no apo-crystals of hArg I were further observed even after the extended time period.

7.5.6.1 Data collection

Frozen hArg I co-crystals (with compounds **1b**, **1b**-1 or **1b**-2) were shipped to PETRA III Synchrotron (DESY, Hamburg) using dry-shipping cryo-container (Taylor-Wharton) and a 1.8 - 2.0 Å data sets were collected at 100 K in the nitrogen stream at the P11 beamline. Initial characterization of the crystals and the optimization of data collection parameters were performed using *XDSapp*.[43] The space group of all hArg I crystals was calculated to be trigonal P3. Software analysis predicted possible twinning for datasets hArg I-**1b**-1 and hArg I-**1b**-2. The data were processed using the *XDS* software.[44] The data collection and processing statistics are reported in Table 7.7.

7.5.6.2 Data processing and refinement

The structures of hArg I co-crystals were solved by molecular replacement using *MOLREP* software within the *CCP4* package.[45, 46] The previous X-ray structure of hArg I (2AEB) was used as a search model yielding a solution of two molecules in the asymmetric unit.[47] The model was further optimized using manual rebuilding via *COOT* and refined with *REFMAC* software.[48, 49] The refinement steps were carried out with global NCS restraints including the twin refinement. The structure figures were prepared with *PyMol*.[50]

Table 7.7. Data collection and refinement statistics (values in parentheses are for the highest resolution shell)

Entry	**hArg I–1b (racemic mixture)**	**hArg I–1b**-1	**hArg I-1b**-2
PDB entry	-	-	-
X-ray source	P 11, PETRA III, DESY, Hamburg		

Wavelength (Å)		1.03	
Space group		P3	
Unit-cell parameters	a=b=91.18 Å c=69.71 Å α=β=90º, γ=120º	a=b=91.07 Å c=69.59 Å α=β=90º, γ=120º	a=b=90.60 Å c=69.35 Å α=β=90º, γ=120º
Resolution range (Å)	45.59 – 1.80 (1.84 – 1.80)	19.90 – 1.80 (1.84 – 1.80)	19.90 – 1.80 (1.91 – 1.80)
No. of observations	82222 (12887)	221741 (35803)	221726 (35463)
No. of unique reflections	53460 (8486)	114882 (18479)	83245 (13699)
Multiplicity	1.54 (1.51)	1.93 (1.93)	2.66 (2.59)
Completeness (%)	88.9 (87.2)	95.4 (94.9)	91.8 (93.8)
R_{mes} (%)	7.2 (72.1)	6.1 (89.1)	6.5 (54.6)
Mean $I/\sigma(I)$	7.72 (1.5)	11.92 (1.13)	11.64 (2.17)
Refinement resolution range (Å)	45.59 – 1.80	45.54 – 2.0	19.92 – 1.80
Twining	no	yes	yes
R_{work} (%)	18.27	15.84	11.54
R_{free} (%)	22.25	18.25	13.78
No. of reflections for refinement	50711	41409	56090
$RMSD_{bonds}$ (Å)	0.0168	0.0197	0.0308
$RMSD_{angles}$ (°)	1.805	2.028	2.52
Protein Atoms	4982	4794	4785
Water molecules	228	13	73
Ligand atoms	34	34	34
Ramachandran plot favored (%)	96.80	97.28	97.28
Ramachandran plot allowed (%)	2.56	1.92	1.92
Ramachandran plot outliers (%)	0.64	0.80	0.80

7.6 References

1. Christianson, D. W.; Cox, J. D. *Annu. Rev. Biochem* **1999,** 68, 33-57.
2. Shi, O.; Morris, S. M.; Zoghbi, H.; Porter, C. W.; O'Brien, W. E. *Mol. Cell. Biol.* **2001,** 21, (3), 811-813.

3. Marathe, C. M.; University of California, L. A., *Regulation of Inflammation by Ppars and Lxrs*. University of California, Los Angeles: 2007.
4. Herzfeld, A.; Raper, S. M. *Biochem. J* **1976,** 153, (2), 469-478.
5. Glass, R. D.; Knox, W. E. *J. Biol. Chem.* **1973,** 248, (16), 5785-5789.
6. Kaysen, G. A.; Strecker, H. J. *Biochem. J* **1973,** 133, (4), 779-788.
7. Kim, N. N.; Cox, J. D.; Baggio, R. F.; Emig, F. A.; Mistry, S. K.; Harper, S. L.; Speicher, D. W.; Morris, S. M., Jr.; Ash, D. E.; Traish, A.; Christianson, D. W. *Biochemistry* **2001,** 40, (9), 2678-2688.
8. Colleluori, D. M.; Reczkowski, R. S.; Emig, F. A.; Cama, E.; Cox, J. D.; Scolnick, L. R.; Compher, K.; Jude, K.; Han, S.; Viola, R. E.; Christianson, D. W.; Ash, D. E. *Arch. Biochem. Biophys.* **2005,** 444, (1), 15-26.
9. Zimmermann, N.; King, N. E.; Laporte, J.; Yang, M.; Mishra, A.; Pope, S. M.; Muntel, E. E.; Witte, D. P.; Pegg, A. A.; Foster, P. S.; Hamid, Q.; Rothenberg, M. E. *The Journal of Clinical Investigation* 111, (12), 1863-1874.
10. Opländer, C.; Römer, A.; Paunel-Görgülü, A.; Fritsch, T.; van Faassen, E. E.; Mürtz, M.; Bozkurt, A.; Grieb, G.; Fuchs, P.; Pallua, N.; Suschek, C. V. *Clin. Pharmacol. Ther.* **2012,** 91, (6), 1074-1082.
11. De Boer, J.; Pouw, F. M.; Zaagsma, J.; Meurs, H. *Am. J. Respir. Crit. Care Med.* **1998,** 158, (6), 1784-1789.
12. Santing, R. E.; Meurs, H.; van der Mark, T. W.; Remie, R.; Oosterom, W. C.; Brouwer, F.; Zaagsma, J. *Pulm. Pharmacol.* **1992,** 5, (4), 265-272.
13. Meurs, H.; Schuurman, F. E.; Duyvendak, M.; Zaagsma, J. *Br. J. Pharmacol.* **1999,** 126, (3), 559-562.
14. Ricciardolo, F. L. M.; Zaagsma, J.; Meurs, H. *Expert Opin. Investig. Drugs* **2005,** 14, (10), 1221-1231.
15. Gosens, R.; Roscioni, S. S.; Dekkers, B. G. J.; Pera, T.; Schmidt, M.; Schaafsma, D.; Zaagsma, J.; Meurs, H. *Eur. J. Pharmacol.* **2008,** 585, (2–3), 385-397.
16. Maarsingh, H.; Bossenga, B. E.; Bos, I. S. T.; Volders, H. H.; Zaagsma, J.; Meurs, H. *Eur. Respir. J.* **2009,** 34, (1), 191-199.
17. Cama, E.; Colleluori, D. M.; Emig, F. A.; Shin, H.; Kim, S. W.; Kim, N. N.; Traish, A. M.; Ash, D. E.; Christianson, D. W. *Biochemistry* **2003,** 42, (28), 8445-8451.
18. Meurs, H.; McKay, S.; Maarsingh, H.; Hamer, M. A.; Macic, L.; Molendijk, N.; Zaagsma, J. *Br. J. Pharmacol.* **2002,** 136, (3), 391-398.
19. WU, G.; MORRIS, S. M. *Biochem. J* **1998,** 336, (1), 1-17.

20. Baggio, R.; Elbaum, D.; Kanyo, Z. F.; Carroll, P. J.; Cavalli, R. C.; Ash, D. E.; Christianson, D. W. *J. Am. Chem. Soc.* **1997,** 119, (34), 8107-8108.
21. Collet, S.; Carreaux, F.; Boucher, J.-L.; Pethe, S.; Lepoivre, M.; Danion-Bougot, R.; Danion, D. *J. Chem. Soc., Perkin Trans. 1* **2000**, (2), 177-182.
22. Di Costanzo, L.; Ilies, M.; Thorn, K. J.; Christianson, D. W. *Arch. Biochem. Biophys.* **2010,** 496, (2), 101-108.
23. D'Antonio, E. L.; Christianson, D. W. *Acta Crystallogr. F-Struct. Biol. Cryst. Commun.* **2012,** 68, (8), 889-893.
24. Ilies, M.; Di Costanzo, L.; Dowling, D. P.; Thorn, K. J.; Christianson, D. W. *J. Med. Chem.* **2011,** 54, (15), 5432-5443.
25. Di Costanzo, L.; Pique, M. E.; Christianson, D. W. *J. Am. Chem. Soc.* **2007,** 129, (20), 6388-6389.
26. Golebiowski, A.; Whitehouse, D.; Beckett, R. P.; Van Zandt, M.; Ji, M. K.; Ryder, T. R.; Jagdmann, E.; Andreoli, M.; Lee, Y.; Sheeler, R.; Conway, B.; Olczak, J.; Mazur, M.; Czestkowski, W.; Piotrowska, W.; Cousido-Siah, A.; Ruiz, F. X.; Mitschler, A.; Podjarny, A.; Schroeter, H. *Bioorg. Med. Chem. Lett.* **2013,** 23, (17), 4837-4841.
27. Zakharian, T. Y.; Di Costanzo, L.; Christianson, D. W. *Org. Biomol. Chem.* **2008,** 6, (18), 3240-3243.
28. Zakharian, T. Y.; Di Costanzo, L.; Christianson, D. W. *J. Am. Chem. Soc.* **2008,** 130, (51), 17254-17255.
29. Smoum, R.; Rubinstein, A.; Dembitsky, V. M.; Srebnik, M. *Chem. Rev.* **2012,** 112, (7), 4156-4220.
30. Van Zandt, M. C.; Whitehouse, D. L.; Golebiowski, A.; Ji, M. K.; Zhang, M.; Beckett, R. P.; Jagdmann, G. E.; Ryder, T. R.; Sheeler, R.; Andreoli, M.; Conway, B.; Mahboubi, K.; D'Angelo, G.; Mitschler, A.; Cousido-Siah, A.; Ruiz, F. X.; Howard, E. I.; Podjarny, A. D.; Schroeter, H. *J. Med. Chem.* **2013,** 56, (6), 2568-2580.
31. Dömling, A.; Wang, W.; Wang, K. *Chem. Rev.* **2012,** 112, (6), 3083-3135.
32. Dömling, A. *Chem. Rev.* **2006,** 106, (1), 17-89.
33. Dömling, A.; Ugi, I. *Angew. Chem. Int. Ed.* **2000,** 39, (18), 3168-3210.
34. Zhao, T.; Boltjes, A.; Herdtweck, E.; Domling, A. *Org. Lett.* **2013,** 15, (3), 639-641.
35. Golebiowski, A.; Paul Beckett, R.; Van Zandt, M.; Ji, M. K.; Whitehouse, D.; Ryder, T. R.; Jagdmann, E.; Andreoli, M.; Mazur, A.; Padmanilayam, M.; Cousido-Siah, A.; Mitschler, A.; Ruiz, F. X.; Podjarny, A.; Schroeter, H. *Bioorg. Med. Chem. Lett.* **2013,** 23, (7), 2027-2030.

36. Daghigh, F.; Fukuto, J. M.; Ash, D. E. *Biochem. Biophys. Res. Commun.* **1994,** 202, (1), 174-180.
37. https://pubchem.ncbi.nlm.nih.gov/compound/284#section=Chemical-and-Physical-Properties
38. Studier, F. W. *Protein Expr. Purif.* **2005,** 41, (1), 207-234.
39. Ericson, P. G. P.; Anderson, C. L.; Britton, T.; Elzanowski, A.; Johansson, U. S.; Källersjö, M.; Ohlson, J. I.; Parsons, T. J.; Zuccon, D.; Mayr, G. *Biol. Lett.* **2006,** 2, (4), 543-547.
40. Nettleship, J. E.; Brown, J.; Groves, M. R.; Geerlof, A. *Methods Mol. Biol.* **2008,** 426, 299-318.
41. Laemmli, U. K. *Nature* **1970,** 227, (5259), 680-5.
42. Garman, E. F.; Mitchell, E. P. *J. Appl. Crystallogr.* **1996,** 29, (5), 584-587.
43. Krug, M.; Weiss, M. S.; Heinemann, U.; Mueller, U. *J. Appl. Cryst.* **2012,** 45, 568-572.
44. Kabsch, W. *XDS. Acta Cryst.* **2010a,** D66, 125-132.
45. Vagin, A.; Teplyakov, A. *Acta Crystallogr. D Biol. Crystallogr.* **2010,** 66, (Pt 1), 22-5.
46. Winn, M. D.; Ballard, C. C.; Cowtan, K. D.; Dodson, E. J.; Emsley, P.; Evans, P. R.; Keegan, R. M.; Krissinel, E. B.; Leslie, A. G.; McCoy, A.; McNicholas, S. J.; Murshudov, G. N.; Pannu, N. S.; Potterton, E. A.; Powell, H. R.; Read, R. J.; Vagin, A.; Wilson, K. S. *Acta Crystallogr. D Biol. Crystallogr.* **2011,** 67, (Pt 4), 235-42.
47. Di Costanzo, L.; Sabio, G.; Mora, A.; Rodriguez, P. C.; Ochoa, A. C.; Centeno, F.; Christianson, D. W. *Proc. Natl. Acad. Sci. U. S. A.* **2005,** 102, (37), 13058-13063.
48. Emsley, P.; Lohkamp, B.; Scott, W. G.; Cowtan, K. *Acta Crystallogr. D Biol. Crystallogr.* **2010,** 66, (Pt 4), 486-501.
49. Murshudov, G. N.; Vagin, A. A.; Dodson, E. J. *Acta Crystallographica Section D* **1997,** 53, (3), 240-255.
50. DeLano, W. L. *DeLano Scientific LLC, Palo Alto, California, USA. http://www.pymol.org* **2009**.